Naunyn-Schmiedeberg's Archives of Pharmacology (2018) 391:587–602
https://doi.org/10.1007/s00210-018-1484-6

ORIGINAL ARTICLE

An integrated approach to elucidate signaling pathways of dioscin-induced apoptosis, energy metabolism and differentiation in acute myeloid leukemia

She-Hung Chan[1] · Pi-Hui Liang[2] · Jih-Hwa Guh[2]

Received: 1 August 2017 / Accepted: 25 February 2018 / Published online: 28 March 2018

Abstract

Although the therapeutics have improved the rates of remission and cure of acute myelogenous leukemia (AML) in recent decades, there is still an unmet medical need for AML therapies because disease relapses are a major obstacle in patients who become refractory to salvage therapy. The development of therapeutic agents promoting both cytotoxicity and cell differentiation may provide opportunities to improve the clinical outcome. Dioscin-induced apoptosis in leukemic cells was identified through death receptor-mediated extrinsic apoptosis pathway. The formation of Bak and tBid, and loss of mitochondrial membrane potential were induced by dioscin suggesting the activation of intrinsic apoptotsis pathway. A functional analysis of transcription factors using transcription factor-DNA interaction array and IPA analysis demonstrated that dioscin induced a profound increase of protein expression of CCAAT/enhancer-binding protein α (C/EBPα), a critical factor for myeloid differentiation. Two-dimensional gel electrophoresis assay confirmed the increase of C/EBPα expression. Dioscin-induced differentiation was substantiated by an increase of CD11b protein expression and the induction of differentiation toward myelomonocytic/granulocytic lineages using hematoxylin and eosin staining. Moreover, both glycolysis and gluconeogenesis pathways after two-dimensional gel electrophoresis assay and IPA network enrichment analysis were proposed to dioscin action. In conclusion, the data suggest that dioscin exerts its antileukemic effect through the upregulation of both death ligands and death receptors and a crosstalk activation of mitochondrial apoptosis pathway with the collaboration of tBid and Bak formation. In addition, proteomics approach reveals an altered metabolic signature of dioscin-treated cells and the induction of differentiation of promyelocytes to granulocytes and monocytes in which the C/EBPα plays a key role.

Keywords Dioscin · Leukemia · Death receptor signaling pathway · C/EBPα · Differentiation · Ingenuity pathway analysis

Introduction

Acute myeloid leukemia (AML) is characterized by rapid growth of abnormal white blood cells which start in the bone marrow and interfere with the generation of normal blood cells. It can sometimes spread to important organs in the body such as the brain, spinal cord, lymph nodes, liver and spleen.

✉ She-Hung Chan
sandychan77@gmail.com

✉ Jih-Hwa Guh
jhguh@ntu.edu.tw

[1] Department of Cosmetic Science, Providence University, 200, Sec. 7, Taiwan Boulevard, Shalu Dist, Taichung 43301, Taiwan

[2] School of Pharmacy, National Taiwan University, No.33, Linsen S. Rd., Zhongzheng Dist, Taipei 100, Taiwan

CCAAT/enhancer-binding protein-alpha (C/EBPα) is a key transcription factor in the control of lineage-specific gene expression and cell proliferation in hematopoiesis and is involved in the differentiation of certain blood cells (Rahman et al. 2016; Nerlov 2004; Yoshida et al. 2012). It has been evident that inhibition of C/EBPα expression and disruption of its activity stops the differentiation of myeloid progenitors (Lin et al. 2011). In several AML subtypes, C/EBPα expression is downregulated or mutated, most prominently, in the M2 subtype where C/EBPα mutations are observed in a population of patients, resulting in a blockade of monocytic or granulocytic differentiation (Nerlov 2004). Therefore, the role of C/EBPα during granulocyte differentiation and in serving as a tumor suppressor is critically important, indicating that therapies with an increase of expression and activation of C/EBPα may counteract the disruption of differentiation in AML.

An increase of glycolysis, the breakdown of glucose into pyruvate to generate ATP, is a hallmark of cancer cells and is known as the Warburg effect (Warburg et al. 1927). Several studies have demonstrated moderate to high levels of glycolytic metabolism in AML (Herst et al. 2011; Liu et al. 2013). Moreover, highly glycolytic AML cells are more resistant to apoptosis induced by anti-AML therapy, such as retinoic acid and arsenic trioxide, suggesting potential resistance to induction chemotherapy (Herst et al. 2011; Song et al. 2016). These findings indicate that targeting glycolysis is a viable strategy for modulating chemoresistance in AML (Xu et al. 2005; Song et al. 2016).

Natural products are promising resources for cancer drug discovery (Abdel-Hamid et al. 2017; Tung et al. 2016). Glycosides of spirostan and furostan type steroids, found in a wide variety of plants, have been demonstrated to display anticancer activities against many cancers including cancers of the prostate, breast, lung and liver. Dioscin, a natural spirostan steroid glycoside widely present in the family of *Dioscoreaceae* and *Liliaceae*, has been extensively studied for its anticancer effects in a variety of cancers through caspase-dependent multiple signaling pathways including up-regulation of p53 and Bax, downregulation of Bcl-2, activation of estrogen receptor-β, induction of oxidative stress, mitochondrial stress, p38 mitogen-activated protein kinase (MAPK) and c-Jun N-terminal kinase (JNK) activation, and inhibition of phosphatidyl inositol 3-kinase (PI3K)/Akt and nuclear factor kappa B (NF-κB) activity (Cai et al. 2002; Wang et al. 2014; Zhao et al. 2016a, b; Zhang et al. 2016a, b; Song et al. 2017; Tao et al. 2017). Besides, dioscin has been reported to induce demethylation of DAPK-1 and RASSF-1α genes via the antioxidant capacity to stimulate apoptosis in bladder cancer cells (Zhou et al. 2017). Furthermore, it inhibits TGF-β1-induced epithelial-to-mesenchymal transition, migration and invasion of A549 lung cancer cells (Lim et al. 2017), and inhibits VEGFR2-mediated angiogenesis through the suppression of downstream kinases including Src, FAK, Akt and Erk1/2 (Tong et al. 2014).

In this study, the integrated bioinformatics approach and functional examination have been used in the aid of apoptosis-related protein array, transcription factor (TF)-DNA array, and proteomics studies to delineate dioscin-induced anti-AML effects as well as the mechanisms that are responsible for anti-proliferative, apoptotic and differentiation activities.

Materials and methods

Materials

Iscove's Modified Dulbecco's Medium (IMDM), RPMI 1640 medium, fetal bovine serum (FBS), penicillin, streptomycin, and all other tissue culture reagents were obtained from GIBCO/BRL Life Technologies (Grand Island, NY). The following antibodies were used: anti-mouse and anti-rabbit IgGs, TRAIL, PARP-1, C/EBP-α, caspase-9, -8 and -3, Bid, Bak, GAPDH (Santa Cruz Biotechnology Inc., Santa Cruz, CA), Fas, FasL and caveolin-1 (Transduction Lab, Lexington, KY). CD11b-FITC, 4,6-diamidino-2-phenylindole dihydrochloride (DAPI), JC-1, leupeptin, dithiothreitol, phenylmethyl sulfonylfluoride (PMSF), propidium iodide (PI), all-trans retinoic acid (ATRA) and all of the other chemical reagents were obtained from Sigma-Aldrich (St. Louis, MO).

Cell lines and cell culture

HL-60 (promyelocytic leukemia), CCRF-CEM (T cell acute lymphoblastic leukemia), and Jurkat (T cell acute lymphoblastic leukemia) were from American Type Culture Collection (Rockville, MD). CCRF-CEM and Jurkat cells were cultured in RPMI-1640 medium and HL-60 cells were cultured in Iscove's Modified Dulbecco's Medium (IMDM). All cells were cultured with 10% fetal bovine serum (FBS) (*v*/*v*) and penicillin (100 U/ml)/streptomycin (100 μg/ml). Cultures were maintained in a humidified incubator at 37 °C in 5% CO_2/95% air.

Mitochondrial MTT reduction activity assay

The cells at a density of 3×10^5 cells/ml were cultured at a 24-well plate. After the compound treatment at the mentioned concentrations and times, the mitochondrial MTT reduction activity was assessed. MTT was dissolved in phosphate-buffered saline (PBS) at a concentration of 5 mg/ml and filtered. From the stock solution, 50 μl per 500 μl of medium was added to each well and plates were gently shaken and incubated at 37 °C for 2 h. After the loading of MTT, the medium was replaced with 1 ml of 100% DMSO and was left for 5 to 10 min at room temperature for color development. The 24-well plate was read by enzyme-linked immunosorbent assay reader (570 nm) to get the absorbance density values.

Flow cytometric detection of apoptosis

After the treatment, the cells were harvested, washed twice with ice-cold PBS, fixed with 70% ethanol at 4 °C for 30 min, and washed with ice-cold PBS. The cells were then resuspended with 0.3 ml of PI solution containing Triton X-100 (0.1% *v*/*v*), RNase (100 mg/ml) and PI (80 mg/ml) in the dark. Cells were analyzed with FACScan and CellQuest software (Becton Dickinson, Mountain View, CA). The level of apoptotic cells containing sub-G1 DNA content was determined as a percentage of the total number of cells. In another assay, the cells were stained with FITC-Annexin V/PI using an apoptosis detection kit (BD Pharmingen) according to the manufacturer's protocol. After the incubation at room

temperature for 15 min in the dark, the apoptosis was detected and quantified using flow cytometric analysis.

DNA fragmentation assay

After the treatment, the cells were collected in a buffer containing 20 mM Tris pH 7.0 and 250 mM sucrose on ice. Total DNA was extracted by Genomic DNA kits (Geneaid, Taiwan). DNA was subsequently subjected to electrophoresis on 2% agarose gels containing SYBR1 green I (1:250 dilution of stock in TE buffer) (Molecular Probes, Eugene, OR), and visualized under UV light.

Confocal microscopic examination with DAPI staining

After the treatment, the cells were fixed with 100% methanol at room temperature for 5 min and were incubated in the solution containing 1 μg/ml DAPI for nuclear staining or the indicated antibody for the detection of specific protein. The cells were analyzed using a confocal laser microscopic system (Leica TCS SP2).

Microscopic observation of cell morphology

After the treatment, the cells were collected by centrifugation and resuspended in 200 μl of PreserveCyt solution. The suspension was passed through a Thinprep processing machine, and the cells were collected. The slides were fixed in 95% alcohol and then stained with Wright-Giemsa for 5 min at room temperature. Stained cells from each treatment group were examined under a fluorescence microscope (Olympus, USA).

Human apoptosis antibody array

To investigate the pathways by which dioscin induces apoptosis, we performed a determination of apoptosis-related proteins using an antibody array (human apoptosis antibody array kit, Raybiotech, Norcross, GA, USA) according to the manufacturer's instructions. After the treatment with dioscin, the cells were collected and 300 μg of protein extract from each sample was incubated with the antibody array membrane for 4 h. The membrane was quantified using a Biospectrum AC ChemiHR 40 system (UVP, Upland, CA, USA) and the membrane image file was analyzed using UVP analysis software.

Measurement of mitochondrial membrane potential ($\Delta\Psi_m$)

JC-1 was used to determine$\Delta\Psi_m$. Cells were treated in the absence or presence of the indicated agent. Thirty minutes before the termination of incubation, the cells were incubated with JC-1 (final concentration of 2 μM) at 37 °C for 30 min. The cells were finally harvested and the accumulation of JC-1 was determined using flow cytometric analysis.

Differentiation effect assay

Differentiation effects of dioscin and ATRA were assessed using established morphologic changes using Wright's staining and immunophenotyping with CD11b expression. Expression of the CD11b (Becton–Dickinson, NJ) immunophenotypic marker was monitored. After treatment, the cells were harvested and incubated with the desired antisera for 30 min at 4 °C, then washed twice, and fixed with staining buffer (Becton–Dickinson, NJ) before analysis. For immunofluorescence analysis, following the appropriate incubation step, the fluoresceinated CD11b antibody was incubated at 4 °C for 30 min, followed by washing and fixing. At least, 10^4 cells were analyzed for FACScan and CellQuest software (BD, CA).

Transcription factor-DNA interaction array analysis

Nuclear extracts from cells were prepared with nuclear extract kit (Panomics, Inc., Redwood City, CA) according to the user manual. Protein-DNA interactions were analyzed using a set of biotin-labeled DNA binding oligonucleotides. Nuclear extracts (15 μg) were pre-incubated with biotin-labeled DNA probe to allow formation of protein/DNA complexes. The protein/DNA complexes were separated from the free probes using a spin column separation system (Panomics). The bound probes were extracted and hybridized to an array membrane spotted with 56 different consensus-binding sequences according to the protocol.

Two-dimensional gel electrophoresis (2-DGE)

2-DGE was performed using Amersham Biosciences IPGphor IEF electrophoresis units (Uppsala, Sweden). Protein samples (200 μg) extracted from the cells of untreated or 2 μM dioscin treatment for 24 h were mixed up with equal volume of rehydration buffer (8 M Urea, 20 mM DTT, 0.5% Triton X-100 and 1% IPG buffer). The rehydration step was carried out with precast 13 cm IPG strips for more than 12 h at low voltage of 30 V. IEF was run following a step-wise voltage increase procedure: 500 V and 1000 V for 3 h each and 2000 V for about 16 h. After IEF, the strips were subjected in equilibration buffers (6 M Urea, 50% Glycerol, 2% SDS and 0.5 M Tris-HCl pH 6.8) for 20 min. The strips were then transferred onto the second-dimensional SDS-PAGE that was run on 1.5 mm thick of 15% polyacrylamide gels.

Silver staining

The gels were fixed with 40% ethanol and 10% glacial acetic acid for 30 min, and then incubated in a

sensitizing buffer containing 30% ethanol, 4.1% sodium acetate and 0.2% sodium thiosulfate for 30 min. After washing three times in water for 5 min each, the gels were stained in 0.1% silver nitrate solution containing 0.02% formaldehyde for 40 min. Development was performed for 15 min in a solution consisting of 2.5% sodium carbonate and 0.01% formaldehyde. Ethylenediaminetetraacetic acid solution (1.46%) was used to stop the development and the stained gels were then washed three times in water for 5 min each.

In gel digestion, mass spectrometry analysis, and protein identification

After silver staining, individual protein bands were excised from the gel and digested overnight at 37 °C with trypsin (1 mg/ml; Promega Corporation, Madison, WI), then the tryptic peptide mixture was eluted for 30 min at 4 °C from the gel with 100 ml of 0.1% trifluoroacetic acid (TFA), followed by 100 ml of 0.1% TFA/60% acetonitrile, and the combined extracts lyophilized. The tryptic peptides were resuspended in 0.1% TFA and analyzed by LC-MS/MS using an LTQ-Orbitrap Velos hybrid mass spectrometer (Thermofisher Scientific, Waltham, MA). Peptide separations were performed on-line with MS by nanoflow liquid chromatography (Dionex Ultimate 3000, Dionex Corporation, CA). Samples were injected in a 10-ml volume of starting mobile phase (2% acetonitrile in 0.1% formic acid) at a flow rate of 750 nl/min onto a Nanoacquity LC system with a 75 um × 15 cm C18 column. Samples were loaded for 15 min before switching the sample loop out of the flow path and decreasing the flow to 300 nl/min. The peptides were then separated by elution with a linear gradient of 2–90% acetonitrile in 0.1% formic acid at 300 nl/min in 90 min and injected onto a Thermo Scientific Velos Orbitrap electrospray mass spectrometer running at a resolution of 60,000 for precursors. Data-dependent MS/MS analysis was carried out using Xcalibur MS acquisition software (Xcalibur 2.1, Thermo Fisher Scientific, Waltham, MA). Each scan cycle consisted of a full scan MS acquired in profile mode at 60 K resolution by the Orbitrap analyzer over the mass range 350–1600 m/z, followed by data-dependent MS/MS scans of the 20 most intense peaks. MS/MS spectra were acquired in higher energy collisional dissociation mode with 35% normalized collision energy. Dynamic exclusion was set for 90 s with a 20 ppm window and monoisotopic precursor selection was enabled. Proteins were identified by Mascot search engine (version 2.2.2, Matrix Science) against Swiss-Prot version 43 protein database. The individual score for the MS/MS spectrum of each peptide was more than 20.

Ingenuity pathway analysis (IPA)

A list of dioscin-modulating proteins was uploaded to the Ingenuity Pathway Analysis (IPA) software to investigate the biological networks associated with these proteins (http://www.ingenuity.com). This analysis uses computational algorithms to identify networks consisting of focus proteins (proteins that were present in our list) and their interactions with other proteins ("non-focused") in the knowledge base. Scores were calculated for each network according to the fit of the network to the set of focus proteins and used to rank networks in the Ingenuity analysis. IPA uses the proteins from the highest-scoring network to extract a connectivity pathway that relates candidate proteins to each other based on their interactions. These candidates were shown to be significantly associated with the Function, Disease, and Canonical Pathways. In addition, we also searched for other proteins involved in this network using the build tools of IPA. Significance of the biofunctions and the canonical pathways were tested by the Fisher exact test p value.

Western blotting

After the treatment, cells were harvested, centrifuged, and lysed in 0.1 ml of lysis buffer containing 10 mM Tris–HCl (pH 7.4), 150 mM NaCl, 1 mM ethylene glycol tetraacetic acid, 1% Triton X-100, 1 mM PMSF, 10 mg/ml leupeptin, 10 mg/ml aprotinin, 50 mM NaF and 100 mM sodium orthovanadate. In certain experiment, the nuclear extraction kit (Panomic, Redwood City, CA) was used to separate nuclear and cytosolic fraction. Total protein was quantified, mixed with sample buffer and boiled at 95 °C for 5 min. Equal amount of protein (30 μg) was separated by electrophoresis in a 12% SDS-PAGE, transferred to PVDF membranes and detected with specific antibodies. The immunoreactive proteins after incubation with appropriately labeled secondary antibody were detected with an enhanced chemiluminescence detection kit (Amersham, Buckinghamshire, UK).

Data analysis

Experimental data are presented as the mean ± standard error of the mean (SEM) of three to five independent experiments. Normality and homogeneity of variance assumptions were checked. The statistical analysis was performed using one way analysis of variance (ANOVA) for multiple samples sets. P values less than 0.05 were considered statistically significant. Statistical Package for the Social Sciences version 16.0 (SPSS Inc., Chicago, IL, USA) and GraphPad Prism version 3.0 (GraphPad Software Inc., La Jolla, CA, USA) software were used.

Results

Dioscin displays anti-proliferative and apoptotic activities

HL-60, CCRF-CEM, and Jurkat cells were used to determine the anti-proliferative and apoptotic activity of dioscin. The data showed that dioscin induced concentration-dependent inhibition of cell survival with IC_{50} values at low micromolar concentrations (Fig. 1a). Flow cytometric analysis of DNA staining showed that dioscin induced both concentration- and time-dependent increase of hypodiploid (sub-G1) DNA content in HL-60 (Fig. 1b and c). Dioscin-induced apoptosis was validated using DNA fragmentation assay (Fig. 1d), revealing that dioscin effectively induced programmed cell death in leukemic cells.

Dioscin induces the activation of TNF-receptor family and extrinsic apoptosis pathway

A differentiation block and an accumulation of immature myeloid cells characterize AML. Induction of apoptosis and differentiation by dioscin has been studied on the focus of anti-AML using AML cell line HL60, a good model for studying growth control and differentiation (Burmistrova et al. 2015; Masuda et al. 2015; Shen et al. 2011). After exposure of HL-60 cells to dioscin for 24 h, the cells were lysed and 43 apoptosis-related proteins were examined using a human apoptosis antibody array kit. As a result, several pro-apoptotic proteins including extrinsic apoptosis pathway related death ligands (e.g., tumor necrosis factor α (TNF-α) and Fas ligand (FasL)) and receptors (e.g., death receptor 6 (DR6), TNF-related apoptosis-inducing ligand (TRAIL) receptor, TNF-R1 and TNF-R2) were upregulated (Fig. 2a). Of note, the protein expressions of both cIAP-2 and CD40 also were increased (Fig. 2a). Most TNF receptors require specific adaptor protein such as Fas-Associated protein with Death Domain (FADD), TNFR-associated death domain (TRADD), receptor-interacting protein 1 (Rip1) and TNF receptor-associated factor 2 (TRAF2) for stimulating downstream signaling, cIAP-2 and CD40 are able to interact with the adaptor protein, serving as mediators of the signal transduction (Baker and Reddy 1998; Varfolomeev et al. 2008). The data indicate that dioscin induces the activation of TNF-receptor superfamily. Next, the IPA software was used to determine whether the dioscin-modulating proteins could be grouped into different functional classes. The top ten canonical signaling pathways activated by dioscin were listed and the death receptor signaling was identified as the most relevant signaling pathway (Fig. 2b).

Dioscin induces apoptosis through extrinsic and intrinsic apoptotic pathways

Several death ligands (e.g., FasL and TRAIL), death receptors (e.g., Fas) and the signals involved in extrinsic apoptotic pathways (caspase-8 and Bid) were studied. The data demonstrated that dioscin induced a significant increase of these signal proteins in a time-dependent manner (Fig. 3a). Because Bid/tBid (truncated Bid) was a key protein required in the crosstalk between extrinsic and intrinsic pathways, the activation of intrinsic pathway was examined. As a result, dioscin induced the loss of mitochondrial membrane potential (Fig. 3b) and activation of caspase-9, a key initiator caspase in intrinsic pathway (Fig. 3a), suggesting the activation of this pathway. The activation of caspases, including caspase-8, -9 and -3, by dioscin in HL-60 cells was similar to previous report (Wang et al. 2014). Notably, the Bak expression was significantly upregulated by dioscin in the present study (Fig. 3a). It has been documented that Bid preferentially activates Bak to ensure cell death through mitochondrial dysfunction and to reach death ligand-mediated maximal induction of apoptosis (Sarosiek et al. 2013). The Bak activation was probably attributed to Bid stimulation.

Identification of multiple transcription factors regulated by dioscin

In addition to induction of apoptosis, the differentiation therapy has been considered as a promising approach for the treatment of AML. The emerging evidence shows that differentiation-based approach to target AML is a potential strategy. Transcription factors play a major role in differentiation in a number of cell types, including various hematopoietic lineages and leukemogenesis (Ohlsson et al. 2016). It is important to identify and characterize the transcription factors that specifically activate important genes in the myeloid lineage. A functional analysis of transcription factors was performed that HL-60 cells were exposed to dioscin, rendering to protein/DNA array that permits profiling DNA binding activities of 54 transcription factors (TF). The signal intensities revealed in the membrane array and reflected the TFs binding activity. The purity of different cellular fractions was confirmed by probing each fraction for corresponding subcellular marker proteins. As shown in Fig. 4, the cytoplasmic marker glyceraldehyde 3-phosphate dehydrogenase (GAPDH) primarily localized in the cytoplasmic fraction, whereas the nuclear marker nucleolin mainly resided in the nuclear fraction, confirming the success of nuclear fractionation. The data showed that several TFs binding activities were

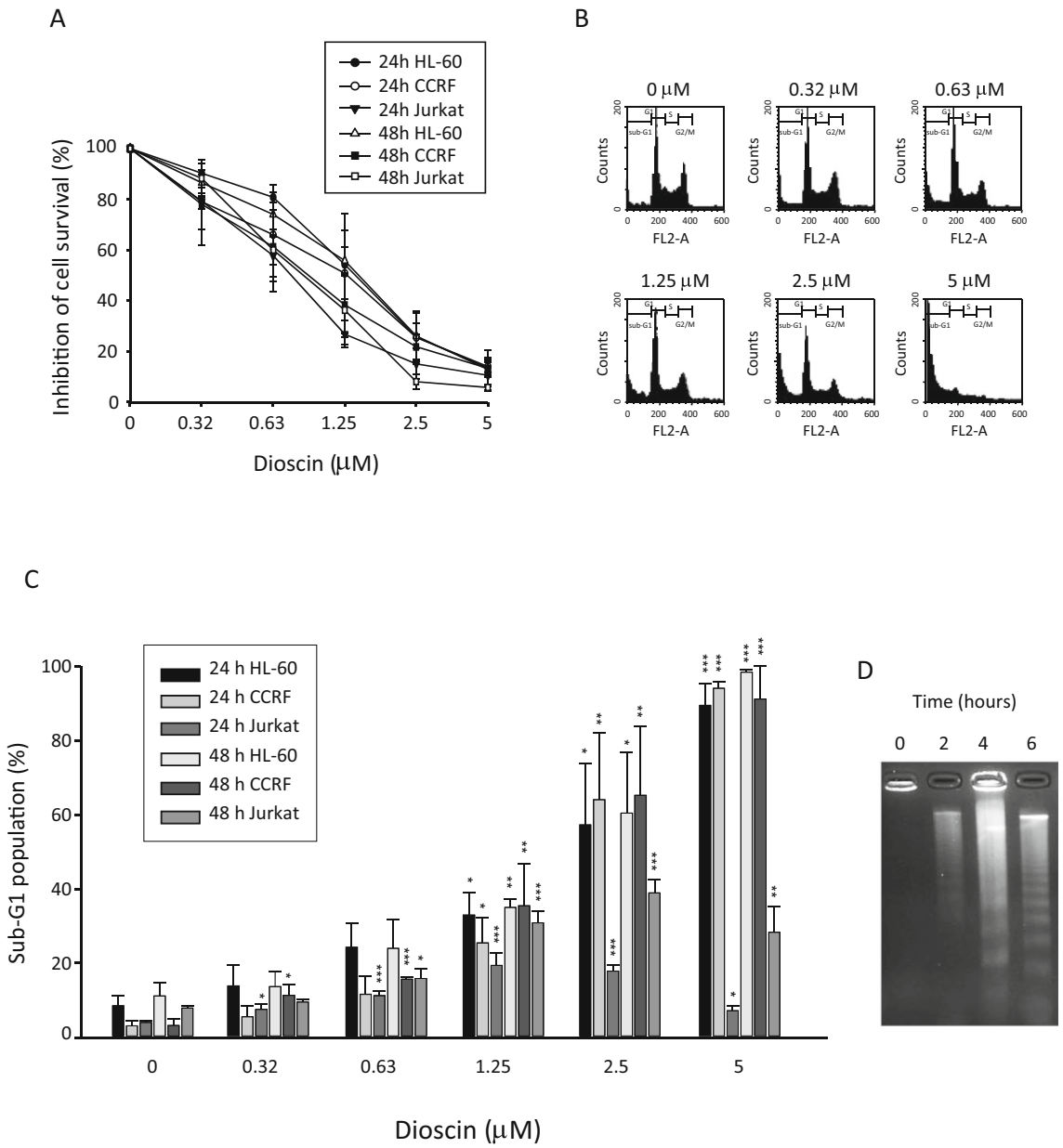

Fig. 1 Identification of apoptotic effect. **a** Graded concentrations of dioscin were added to the cells for 24 or 48 h. The cytotoxic effect was determined by MTT assay. **b** HL-60 cells were treated in the absence or presence of dioscin for 24 h. After the treatment, the cells were fixed and stained with propidium iodide to analyze DNA content by FACScan flow cytometer. **c** Quantitative analysis of sub-G1 (apoptosis) population using flow cytometric analysis of propidium iodide staining. **d** HL-60 cells were treated with 2 μM dioscin for 2, 4, and 6 h. Total DNA was extracted and subjected to electrophoresis for the detection of DNA fragmentation. Data are expressed as mean ± SEM of three to five independent experiments. $*P < 0.05$, $**P < 0.01$, and $***P < 0.001$ compared with the control

increased by dioscin, including Myc/Max, MRE, p53, smad/SBE, and SRE; whereas, those of GR/PR, Brn-3 and AR were decreased. Furthermore, the IPA software generated top ten canonical signaling pathways listed in Fig. 5a, which highlighted several probable pathways including glucocorticoid receptor signaling, Toll-like receptor signaling, PXR/RXR activation, and acute myeloid leukemia signaling of target cells. Accordingly, the key signal that was cross-reacted by these pathways was explored (Fig. 5b). Increasing lines of evidence have demonstrated that glucocorticoid receptor can regulate gene expression by interacting with CCAAT/enhancer-binding protein α (C/EBPα) (Muratcioglu et al. 2015). Several toll-like receptor agonists can downregulate C/EBPα expression, leading to increased expressions of several genes responsible to a variety of neurological disorders (Ejarque-Ortiz et al. 2007). More importantly, the variant fusion proteins, promyelocytic leukemia zinc finger-retinoic acid receptor α (PLZF-RARα), have been identified to inhibit myeloid cell differentiation

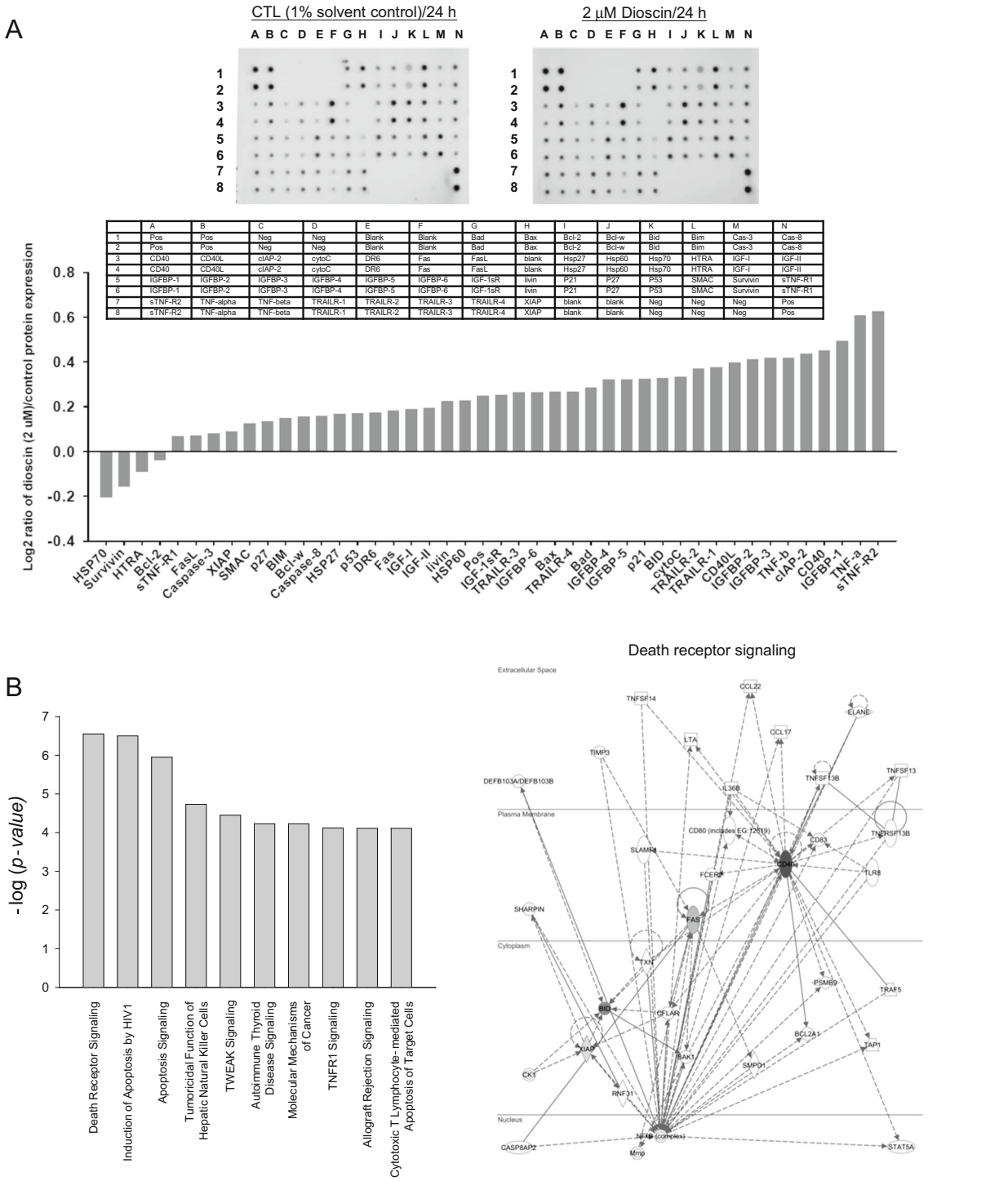

	A	B	C	D	E	F	G	H	I	J	K	L	M	N
1	Pos	Pos	Neg	Neg	Blank	Blank	Bad	Bax	Bcl-2	Bcl-w	Bid	Bim	Cas-3	Cas-8
2	Pos	Pos	Neg	Neg	Blank	Blank	Bad	Bax	Bcl-2	Bcl-w	Bid	Bim	Cas-3	Cas-8
3	CD40	CD40L	cIAP-2	cytoC	DR6	Fas	FasL	blank	Hsp27	Hsp60	Hsp70	HTRA	IGF-I	IGF-II
4	CD40	CD40L	cIAP-2	cytoC	DR6	Fas	FasL	blank	Hsp27	Hsp60	Hsp70	HTRA	IGF-I	IGF-II
5	IGFBP-1	IGFBP-2	IGFBP-3	IGFBP-4	IGFBP-5	IGFBP-6	IGF-1sR	livin	P21	P27	P53	SMAC	Survivin	sTNF-R1
6	IGFBP-1	IGFBP-2	IGFBP-3	IGFBP-4	IGFBP-5	IGFBP-6	IGF-1sR	livin	P21	P27	P53	SMAC	Survivin	sTNF-R1
7	sTNF-R2	TNF-alpha	TNF-beta	TRAILR-1	TRAILR-2	TRAILR-3	TRAILR-4	XIAP	blank	blank	Neg	Neg	Neg	Pos
8	sTNF-R2	TNF-alpha	TNF-beta	TRAILR-1	TRAILR-2	TRAILR-3	TRAILR-4	XIAP	blank	blank	Neg	Neg	Neg	Pos

Fig. 2 Protein array analysis and the ingenuity pathway analysis. HL-60 cells were incubated in the absence or presence of dioscin (2 μM) for 24 h. The cells were lysed and equal amount of protein from each sample was used for the assay. **a** Quantitative analysis in the arrays showed differences in the apoptotic marker proteins. All the protein levels have been normalized in the positive dots. **b** The ingenuity pathway analysis (IPA) software was used to determine the top ten canonical signaling pathways activated by dioscin

through associating with C/EBPα and inhibiting its activity (Girard et al. 2013). Therefore, C/EBPα has been considered as a cellular target if differentiation occurs under dioscin treatment. As a consequence, dioscin led to a profound increase of protein expression of C/EBPα (Fig. 5c).

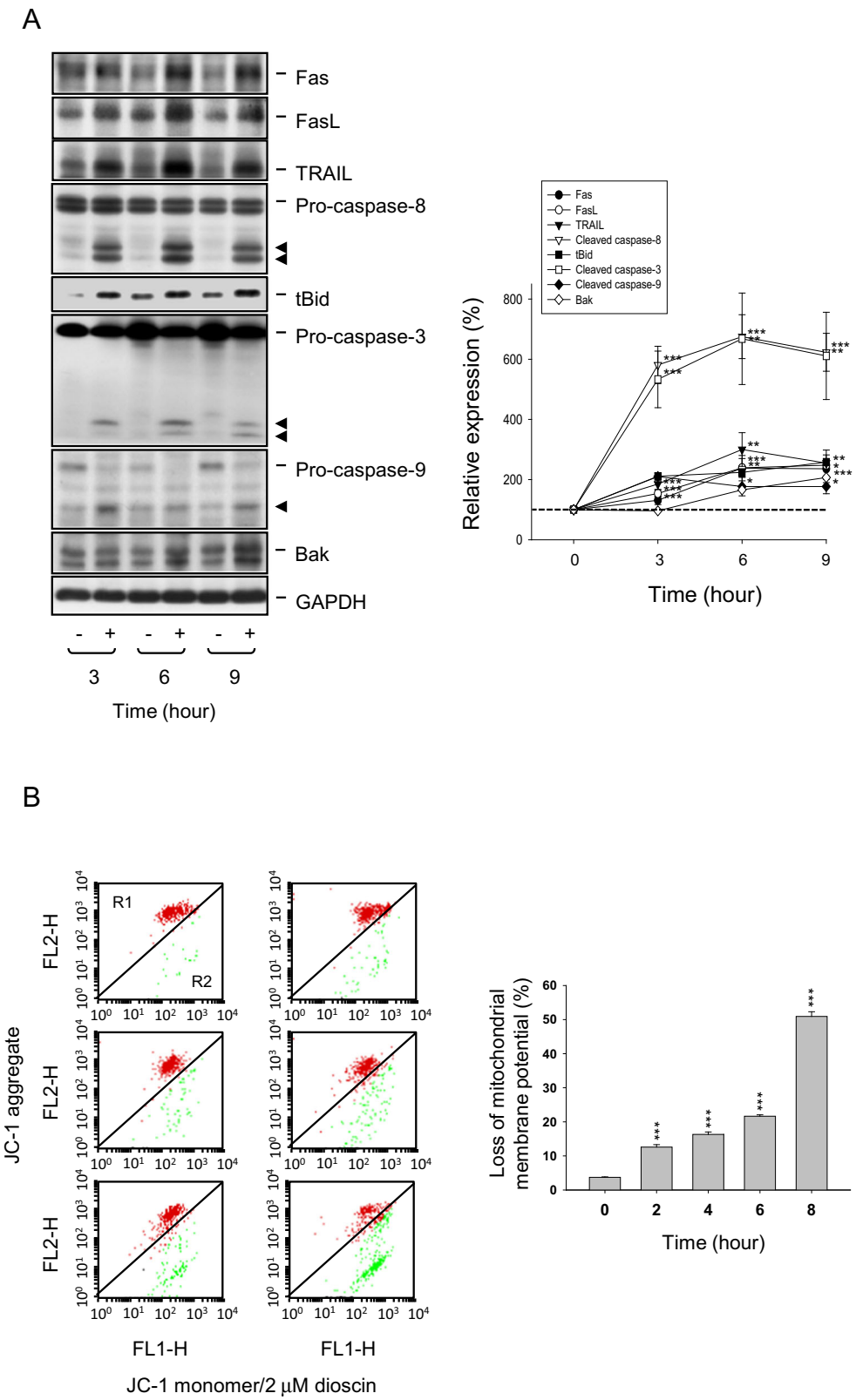

Fig. 3 Effect of dioscin on death receptor signaling and mitochondrial membrane potential. HL-60 cells were incubated in the absence or presence of dioscin (2 μM) for the indicated times. **a** The cells were harvested for the detection of protein expression using Western blotting or **b** the cells were incubated with JC-1 dye for the detection of mitochondrial membrane potential using flow cytometric analysis. Data are expressed as mean ± SEM of three to four independent experiments. $^{*}P < 0.05$, $^{**}P < 0.01$, and $^{***}P < 0.001$ compared with the control

	1	2	3	4	5	6	7	8	9	10	11	12	13	14	15	16	17	18	
A	AP-1	AP-1	AP-2	AP-2	AR	AR	Brn-3	Brn-3	CEBP	CEBP	CBF	CBF	CDP	CDP	c-Myb	c-Myb	AP-1	AP-1	A
B	AP-1	AP-1	AP-2	AP-2	AR	AR	Brn-3	Brn-3	CEBP	CEBP	CBF	CBF	CDP	CDP	c-Myb	c-Myb	AP-1	AP-1	B
C	CREB	CREB	E2F1	E2F1	EGR	EGR	ER	ER	Ets	Ets	Ets-1/Pea-3	Ets-1/Pea-3	FAST-1	FAST-1	GAS/ISRE	GAS/ISRE	AP-2	AP-2	C
D	CREB	CREB	E2F1	E2F1	EGR	EGR	ER	ER	Ets	Ets	Ets-1/Pea-3	Ets-1/Pea-3	FAST-1	FAST-1	GAS/ISRE	GAS/ISRE	AP-2	AP-2	D
E	GATA	GATA	GR/PR	GR/PR	HNF-4	HNF-4	IRF-1	IRF-1	MEF-1	MEF-1	MEF-2	MEF-2	Myc/Max	Myc/Max	NF-1	NF-1			E
F	GATA	GATA	GR/PR	GR/PR	HNF-4	HNF-4	IRF-1	IRF-1	MEF-1	MEF-1	MEF-2	MEF-2	Myc/Max	Myc/Max	NF-1	NF-1			F
G	NFAT-1	NFAT-1	NF-E1/YY1	NF-E1/YY1	NF-E2	NF-E2	NFκB	NFκB	OCT	OCT	p53	p53	Pax-5	Pax-5	Pbx-1	Pbx-1			G
H	NFAT-1	NFAT-1	NF-E1/YY1	NF-E1/YY1	NF-E2	NF-E2	NFκB	NFκB	OCT	OCT	p53	p53	Pax-5	Pax-5	Pbx-1	Pbx-1			H
I	Pit-1	Pit-1	PPAR	PPAR	PRE	PRE	RAR (DR5)	RAR (DR5)	RXR(DR-1)	RXR(DR-1)	SIE	SIE	Smad SBE	Smad SBE	Smad 3/4	Smad 3/4			I
J	Pit-1	Pit-1	PPAR	PPAR	PRE	PRE	RAR (DR5)	RAR (DR5)	RXR(DR-1)	RXR(DR-1)	SIE	SIE	Smad SBE	Smad SBE	Smad 3/4	Smad 3/4			J
K	Sp 1	Sp 1	SRE	SRE	Stat 1	Stat 1	Stat 3	Stat 3	Stat 4	Stat 4	Stat 5	Stat 5	Stat 6	Stat 6	TFIID	TFIID			K
L	Sp 1	Sp 1	SRE	SRE	Stat 1	Stat 1	Stat 3	Stat 3	Stat 4	Stat 4	Stat 5	Stat 5	Stat 6	Stat 6	TFIID	TFIID			L
M	TR	TR	TR (DR4)	TR (DR4)	USF-1	USF-1	VDR (DR3)	VDR (DR3)	HSE	HSE	MRE	MRE							M
N	TR	TR	TR (DR4)	TR (DR4)	USF-1	USF-1	VDR (DR3)	VDR (DR3)	HSE	HSE	MRE	MRE							N
O																			O

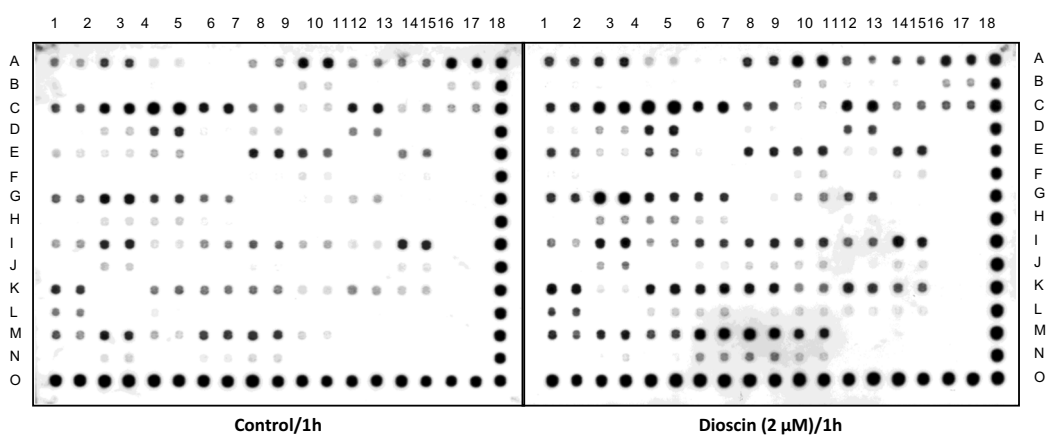

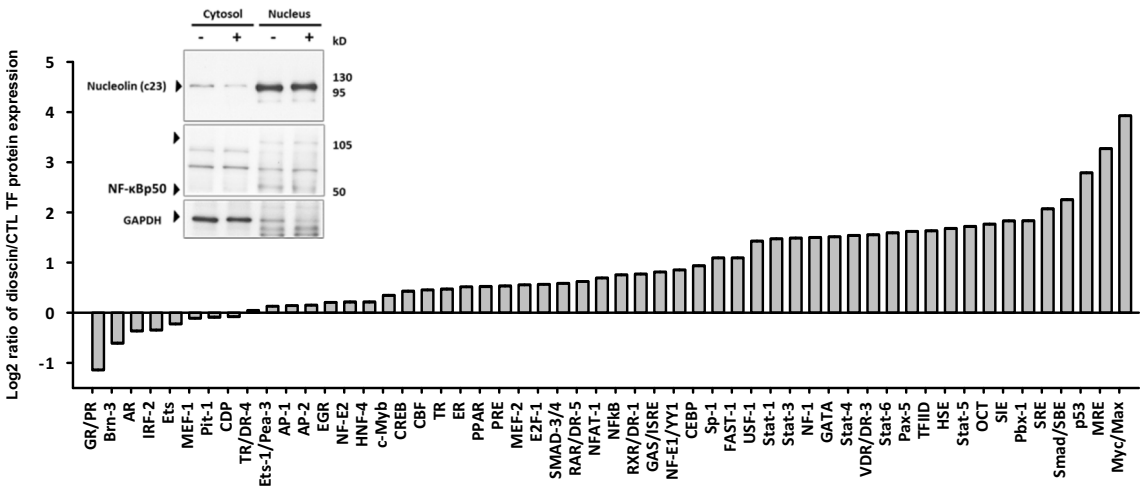

Fig. 4 Effect of dioscin on the activation of transcription factor. HL-60 cells were incubated in the absence or presence of dioscin (2 μM) for 1 h. The nuclear extracts were prepared and preincubated with biotin-labeled DNA probe to allow formation of protein/DNA complexes. The protein/DNA complexes were separated from the free probes using a spin column separation system. The bound probes were extracted and hybridized to an array membrane spotted with 56 different consensus-binding sequences according to the protocol

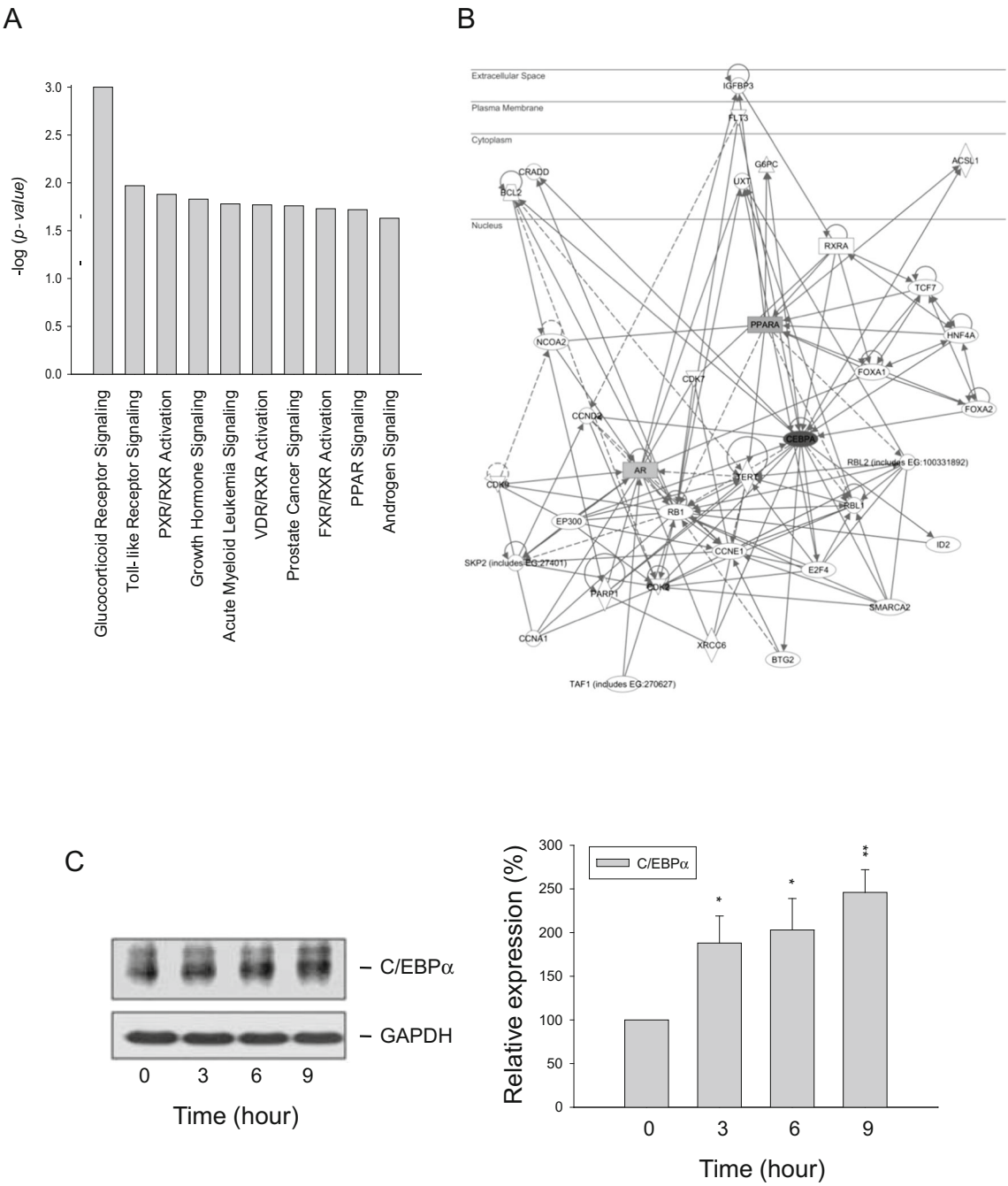

Fig. 5 Determination of canonical pathways from transcription factor-DNA array activated by dioscin-treated in HL-60 cells. **a** Top ten transcription factor canonical signaling pathways activated by dioscin demonstrated in Fig. 4. **b** The ingenuity pathway analysis (IPA) software was used to determine the canonical signaling pathways. **c** The cells were treated with or without dioscin (2 μM) for the indicate times. After the treatment, the cells were harvested for the detection of protein expression using Western blotting. The data have been normalized with the internal control of GAPDH expression and have been demonstrated relative to zero hour. Data are expressed as mean ± SEM of three independent experiments. $^{*}P < 0.05$, $^{**}P < 0.01$, and $^{***}P < 0.001$ compared with the zero hour control

Dioscin induces myelomonocytic differentiation of AML cells

A block in terminal myeloid differentiation is a hallmark of myeloid leukemia cells. To investigate the potential role of dioscin in myeloid cell differentiation, especially in promyeloid stage, the expression of cell surface CD11b during HL-60 differentiation was examined. Dioscin-induced increase of CD11b protein expression was detected by immunostaining (Fig. 6a) and the differentiation toward myelomonocytic/granulocytic lineages was further confirmed based on hematoxylin and eosin staining and CD11b staining (Fig. 6b). Flow cytometric analysis of cell

surface CD11b expression showed that both dioscin and ATRA significantly increased the expression levels (Fig. 6c and d).

Identification of differentially expressed proteins in dioscin-treated HL-60 cells

To elucidate the differentially expressed proteins in dioscin-treated HL-60 cells, the in-gel digestions and LC-MS/MS were performed to identify proteins responsible for dioscin treatment. The analyses identified 43 differentially expressed proteins after an 8-h dioscin treatment; the names of these 43 proteins, their accession numbers in the Swiss-Port database, molecular mass, Mascot score, percentage of coverage, and their identities as well as quantitative data were summarized (Table 1). The assay also demonstrated an upregulation of C/EBPα expression to dioscin action (Table 1). Moreover, several canonical signaling pathways responded to dioscin were proposed, including glycolysis and gluconeogenesis pathways, after IPA network enrichment analysis (Fig. 7). Cellular metabolic state and individual metabolites have been suggested to regulate various cellular functions, including apoptosis and differentiation of functional phenotype of immune cells (Suzuki et al. 2016). The modification of glycolysis and gluconeogenesis pathways by dioscin might, therefore, reinforce its impact on both cell apoptosis and differentiation.

Discussion

Owing to pharmacological significance, the steroidal saponins have caught the attention of phytochemists, biologists and drug discovery scientists. Recently intensive research has been focused on exploring saponins for anticancer therapies. Dioscin is one of the most common steroidal saponins, displaying convincing anticancer activity in several human cancer cells through apoptosis-inducing pathways (Wang et al. 2014; Zhao et al. 2016a; Zhang et al. 2016a, b). The present study has elucidated functionally significant interactions in dioscin-treated leukemic cells on transcription and proteome levels, assisting to understand both the role of individual interacting partners and the order of cascade protein interrelations in cellular regulatory and signaling pathways of both apoptosis and differentiation.

Apoptosis and differentiation machineries play a crucial role in hematopoietic cell homeostasis. A number of hematological diseases involve a deregulation of these machineries. The therapeutic strategy, therefore, is developed to restore the normal function of these machineries. The extrinsic apoptotic pathway is initiated by death receptor activation, leading to the formation of death receptor signaling platforms and activation of caspase-8 mediated cell killing (Lavrik 2014). Death receptors (e.g., TNFR1, DR4, DR5 and Fas) are cell surface receptors transmitting apoptotic signals initiated by individual ligand, such as TNF-α, TRAIL and FasL (CD95L). They can activate a caspase cascade and induce apoptosis very rapid upon ligand binding. Notably, it has been suggested that the sensitivity of leukemic cells to apoptosis is increased in a death receptor-dependent manner (Zheng et al. 2013). Apoptosis antibody array and Ingenuity Pathway Analysis (IPA) revealed that death receptor signaling pathway was identified as the highest-ranked molecular and cellular function upon dioscin-induced effects. Western blot analysis also validated the upregulation of death receptors and the ligands, and the downstream caspase activation. Similar studies have been reported by Kim and the colleagues (Kim et al. 2012). Importantly, dioscin induced a significant increase of tBid formation, a unique pro-apoptotic Bcl-2 family members integrating both the extrinsic and intrinsic pathways (Katz et al. 2012; Tiwari et al. 2015). Recent studies on structural and molecular levels of mitochondria and tBid protein have revealed that mitochondrial carrier homolog 2 participates in recruiting tBid to the mitochondria, where it activates apoptosis (Katz et al. 2012). Our data demonstrated a time-dependent loss of mitochondrial membrane potential and activation of caspase-9, confirming the crosstalk between both extrinsic and intrinsic apoptosis pathways to dioscin action. In addition, another pro-apoptotic Bcl-2 relative, Bak, was activated by dioscin. Bak is a key player to permeabilize mitochondrial outer membrane during the intrinsic apoptosis pathway. It converts to active form through undergoing a large conformational change to form apoptotic pores in mitochondrial outer membrane that allows the release of cytochrome *c* and other proteins to promote caspase activity to kill the cell. Because Bid has been suggested to preferentially activate Bak to ensure cell death through mitochondrial dysfunction (Sarosiek et al. 2013), our data suggest that dioscin efficiently induces caspase-dependent apoptosis through a crosstalk between extrinsic and intrinsic apoptosis pathways. In addition to caspase-dependent pathway in leukemia cells, dioscin also has been reported to induce cell death via apoptosis inducing factor (AIF) involved caspase-independent pathway in breast cancer cells (Kim et al. 2014).

Clinically effective differentiation therapy has been demonstrated in acute myelogenous leukemia. Recently, dioscin has been reported to induce differentiation of chondrocytes and osteoblasts through LDL related protein 5 and estrogen receptor pathway (Zhang et al. 2014; You et al. 2016). In contrast, it suppressed osteoclast differentiation through the inhibition of Akt activation (Qu et al. 2014). However, the effects of dioscin on leukemia differentiation and mechanism study are scarcely reported. C/EBPα is an important transcription factor in the regulation of lineage-specific gene expression and cell proliferation in hematopoiesis and is involved in the differentiation of certain blood cells (Nerlov 2004; Yoshida et al. 2012). It has been demonstrated that inhibition of C/EBPα expression and disruption of its activity stops the differentiation of myeloid progenitors (Lin et al. 2011). Consistent with its importance in normal myeloid differentiation, expression and activity of C/EBPα

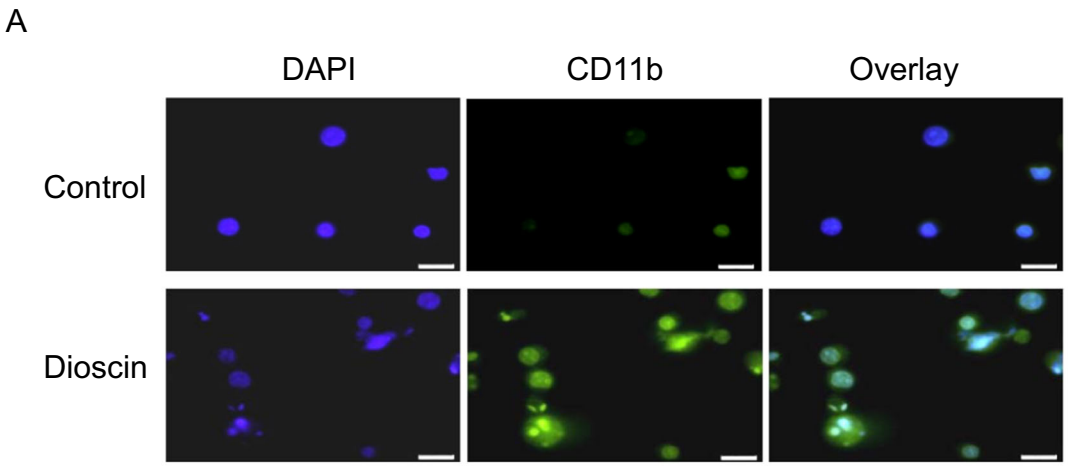
A
DAPI
CD11b
Overlay
Control
Dioscin

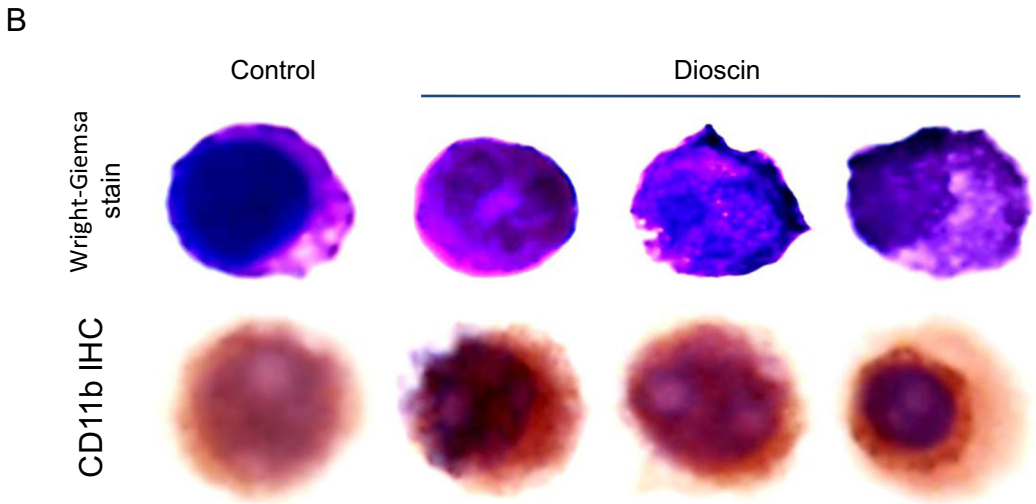
B
Control
Dioscin
Wright-Giemsa stain
CD11b IHC

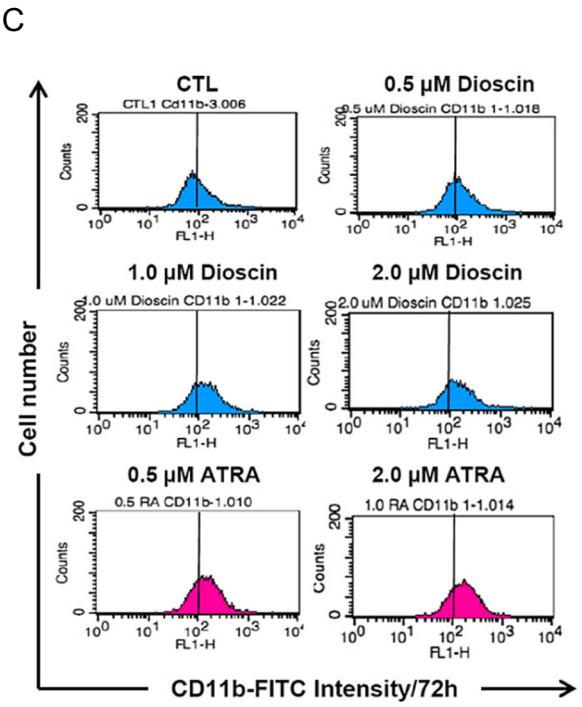
C
CTL
CTL1 Cd11b-3.006
0.5 μM Dioscin
0.5 uM Dioscin CD11b 1-1.018
1.0 μM Dioscin
1.0 uM Dioscin CD11b 1-1.022
2.0 μM Dioscin
2.0 uM Dioscin CD11b 1.025
0.5 μM ATRA
0.5 RA CD11b-1.010
2.0 μM ATRA
1.0 RA CD11b 1-1.014
Counts
FL1-H
Cell number
CD11b-FITC Intensity/72h

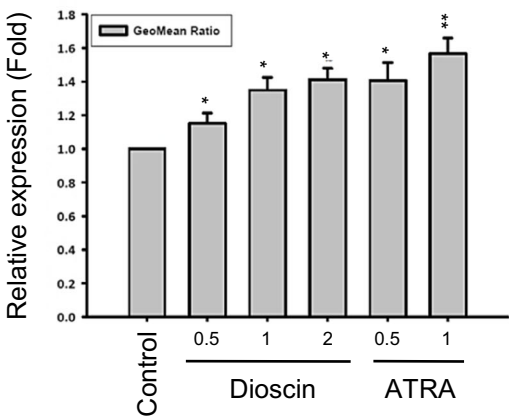
D
GeoMean Ratio
Relative expression (Fold)
Control
0.5
1
2
0.5
1
Dioscin
ATRA

◀ **Fig. 6** Effect of dioscin on cell differentiation. **a**, **b** HL-60 cells were incubated in the absence or presence of dioscin (2.0 μM) for 72 h, or **c**, **d** the cells were incubated with the indicated compound for 72 h. **a** The immunofluorescence staining with CD11b-FITC was performed. The nuclei were stained with DAPI. Bar, 20 μl. **b** Wright-Giemsa staining and immunohistochemical staining of CD11b were performed. **c** The cells were incubated with FITC-conjugated anti-CD11b mouse antibody and analyzed by flow cytometry. **d** The quantitative analysis was performed. Data are expressed as mean ± SEM of three independent experiments. $^{*}P < 0.05$ and $^{**}P < 0.01$ compared with the control

are impaired in several types of myeloid leukemia by various mechanisms, such as transcriptional silencing, translational inhibition, posttranslational modification, decrease in DNA binding, or point mutations resulting in increased production of a dominant negative form) (Tenen 2003; Radomska et al. 2015). AML is characterized by a block in differentiation along one or more hematopoietic lineage. It has been well identified that C/EBPα is mutated in many AML samples examined and most prominently in the promyeloid leukemia cell type (Nerlov 2004). Accordingly, re-introduction of C/

Table 1 Identification of differently expressed proteins between control and dioscin-treated HL-60 cells

Spot no.	Official symbol	NCBI accession no.	Protein hits name	MW (kDa)	Mascot scores	Match peptides	Protein coverage (%)	Dioscin/CTL fold change
21–28	EEF1A1	gi|927065	Eukaryotic translation elongation factor 1 alpha 1-like 14	42.79	52	1	1	5.13
18–21	EEF1A1	gi|181967	Elongation factor 1-alpha	35.20	104	5	2	2.69
13–17	TPI1	gi|136066	Triosephosphate isomerase	26.60	50	3	2	2.53
4–25	NAA38	gi|7706425	N-alpha-acetyltransferase 38	10.39	58	2	2	2.37
9–18	PGK1	gi|4505763	Phosphoglycerate kinase 1	44.58	51	3	3	2.27
8–23	HMG-1L10	gi|20138433	Putative high mobility group protein 1-like 10	24.20	133	8	25	2.12
6–10	CALR	gi|4757900	Calreticulin precursor	48.11	183	8	7	2.1
6–10	CALR	gi|325533983	Calreticulin	30.09	192	8	7	2.1
11–25	CFL-1	gi|5031635	Cofilin-1	18.49	69	4	3	2.07
3–11	PDHB	gi|291084858	Pyruvate dehydrogenase E1 component subunit beta, mitochondrial isoform 2 precursor	37.49	67	3	3	1.94
3–11	CAPZA1	gi|5453597	F-actin-capping protein subunit alpha-1	32.90	131	7	4	1.94
18–20	EF1A	gi|181967	Elongation factor 1-alpha	35.20	74	7	2	1.91
16–10	PGK1	gi|4505763	Phosphoglycerate kinase 1	44.58	271	13	10	1.77
16–24	CEBPA	gi|440306	CCAAT/enhancer binding protein	22.11	104	3	3	1.76
16–10	TALDO1	gi|5803187	Transaldolase	37.51	148	5	5	1.34
19–25	HINT1	gi|4885413	Histidine triad nucleotide-binding protein 1	13.79	99	3	3	1.07
19–25	PRKCI	gi|227968190	Pkci-1-Zinc	13.77	99	3	3	1.07
18–14	HMGB1	gi|55958714	High-mobility group box 1	18.79	121	4	4	0.96
19–24	RPS12	gi|36146	Ribosomal protein S12	14.51	71	3	2	0.82
21–12	ETFA	gi|2781202	Electron transfer flavoprotein subunit alpha	33.07	123	4	4	0.73
21–12	ALDOA	gi|28595	Aldolase A protein	11.93	64	2	2	0.73
25–13	FBA	gi|4557976	Fructose 1,6-bisphosphate aldolase	39.26	116	3	3	0.72
25–13	EF1A	gi|181967	Elongation factor 1-alpha	35.20	78	6	2	0.72
23–16	GAPDH	gi|31645	Glyceraldehyde 3-phosphate dehydrogenase	36.03	98	6	4	0.7
20–15	TPI1	gi|4507645	Triosephosphate isomerase isoform 1	26.65	402	28	12	0.69
9–7	TUBB	gi|1297274	Beta-tubulin	50.48	289	21	8	0.57
25–22	PPIA	gi|1633054	Cyclophilin A	17.87	109	11	5	0.55
8–6	PDI	gi|20070125	Protein disulfide-isomerase precursor	57.08	619	37	23	0.54
25–25	ACTG1	gi|178045	Gamma-actin 1	25.86	89	2	2	0.49
24–17	PEBP1	gi|913159	Neuropolypeptide h3	20.91	194	11	2	0.48
24–17	PSMB8	gi|596140	Proteasome subunit LMP7	30.41	137	5	5	0.48
24–17	PEBP1	gi|4505621	Phosphatidylethanolamine-binding protein 1	21.04	194	11	5	0.48
21–8	ENO1	gi|4503571	Alpha-enolase isoform 1	47.13	390	18	12	0.41
A4	MIF	gi|1942977	Macrophage migration Inhibitory factor	12.44	106	9	2	0.35
A6	PRDX1	gi|4505591	Peroxiredoxin-1	22.09	106	3		0.15
19–8	ENO1	gi|4503571	Alpha-enolase isoform 1	47.13	346	17	13	0.08
19–7	PKM	gi|35505	Pyruvate kinase	57.84	537	24	14	0.02

HL-60 cells were incubated in the absence or presence of dioscin (2 μM) for 8 h. After the treatment, the cells were harvested and the proteins were separated by 2D gel electrophoresis using 18 cm pH 3–10 NL strip and 14% SDS-PAGE. Proteins were detected by silver staining. These spots were then identified by LC-MS/MS

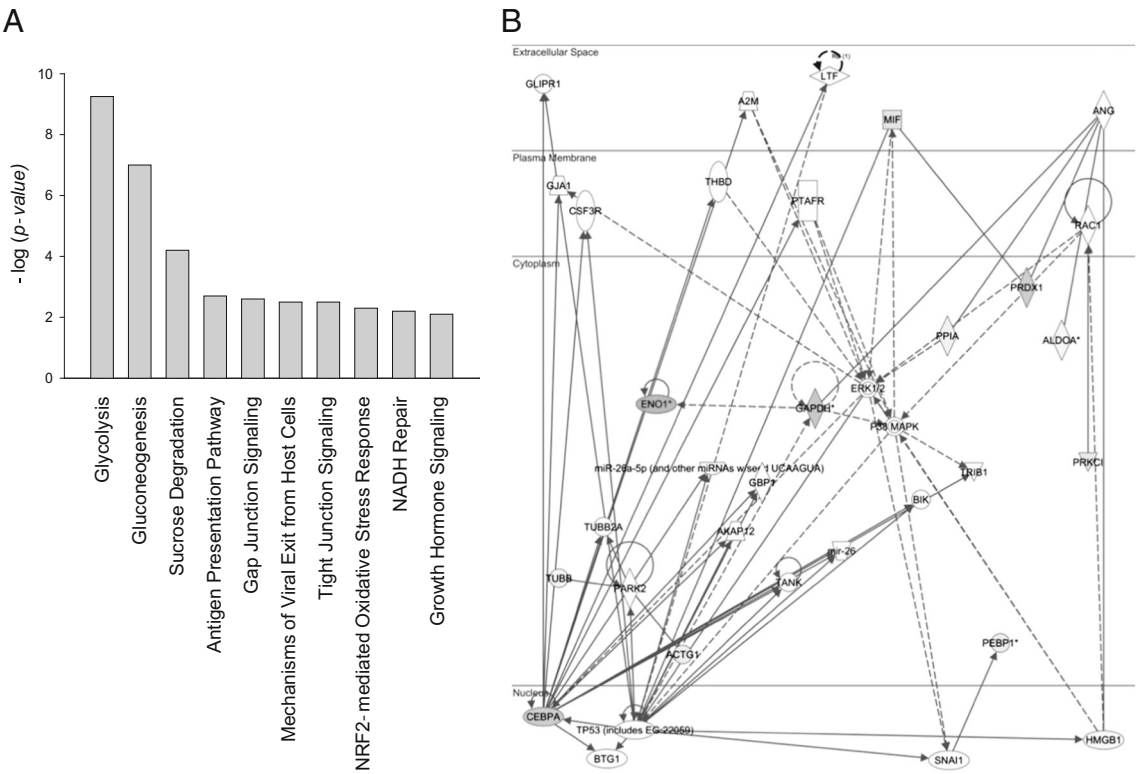

Fig. 7 Determination of canonical pathways from IPA analysis of 2-D gel electrophoresis to identify cellular proteins. **a** The assay was perform as demonstrated in Table 1 and the top ten canonical signaling pathways activated by dioscin were obtained. **b** The ingenuity pathway analysis (IPA) software was used to determine the canonical signaling pathways

EBPα expression and function may prevail against the block of differentiation, leading to apoptosis of leukemic cells and recovery of cells with normal function. Radomska and the colleagues have established a cell-based high throughput screening to identify chemical compounds capable of inducing C/EBPα expression and myeloid differentiation (Radomska et al. 2015). In this study, a protein/DNA array to profile the DNA binding activity of multiple TFs was used and the IPA analysis showed several probable pathways to dioscin action; importantly, C/EBPα plays a common and crucial role in these pathways (Ejarque-Ortiz et al. 2007; Girard et al. 2013; Muratcioglu et al. 2015). The data also revealed that dioscin induced a profound increase of C/EBPα expression and CD11b protein expression (a classical myeloid lineage marker). It also induced the differentiation of HL-60 cells toward myelomonocytic/granulocytic lineages.

It is noteworthy that C/EBPα also plays a role in death receptor involved apoptosis pathway. It has been documented that

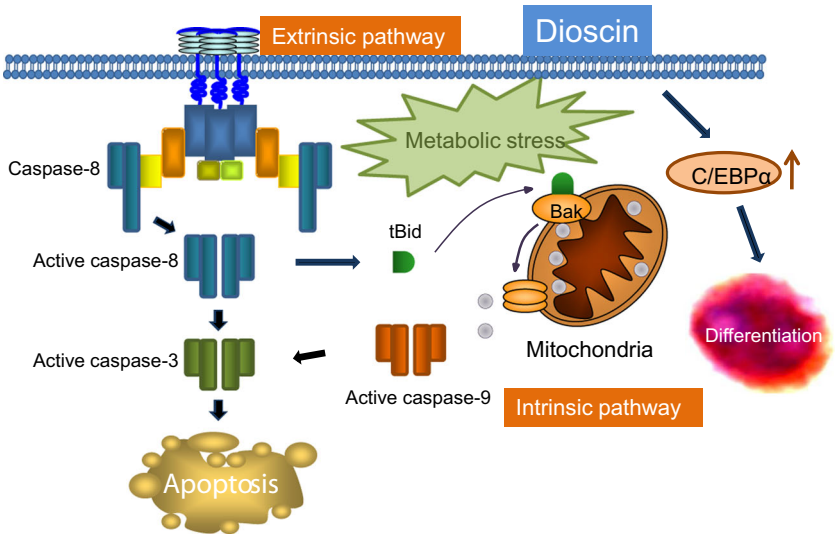

Fig. 8 Schematic figure for dioscin-mediated signaling pathways in HL-60 cells. Dioscin exerts its antileukemic effect through the upregulation of both death ligands and death receptors and a crosstalk activation of mitochondrial apoptosis pathway with the collaboration of tBid and Bak formation. In addition, proteomics approach reveals an altered metabolic signature of dioscin-treated cells and the induction of differentiation of promyelocytes to granulocytes and monocytes in which the C/EBPα plays a key role

the infection of adenovirus vector expressing C/EBPα gene (Ad-C/EBPα) is able to induce apoptosis in various types of cells mainly through death receptor pathways (Wang et al. 2009). Yao and the colleagues have reported that the ectopic overexpression of HMG-box containing protein 1 in myeloid cells induces apoptosis and enhances differentiation through an increase of FasL levels and myeloid-specific transcription factor C/EBPα (Yao et al. 2005). Moreover, CD95/Fas death receptor pathway has been suggested to be an integral part of the apoptotic response associated with the end of the normal terminal myeloid differentiation program. Deregulated c-myc expression can activate this signaling pathway prematurely and C/EBPα has been implicated in the downregulation of c-myc expression (Hoffman et al. 2002). Taken together, these studies suggest that C/EBPα can be a crucial regulator responsible for leukemic apoptosis through death receptor-mediated apoptosis pathway.

The in-gel digestions and LC-MS/MS were performed to identify proteins responsible for dioscin treatment. The IPA network enrichment analysis showed that dioscin might affect the glycolysis and gluconeogenesis pathways in HL-60 cells. Because the concomitant activation or downregulation of glycolysis and gluconeogenesis would cause a metabolic stress, impairing the metabolic rewiring of cancer cells, targeting glycolysis/gluconeogenesis pathways for metabolic reprogramming may be a feasible anticancer strategy (Ma et al. 2013; Khan and Chakrabarti 2015). More than ten protein spots were found to be up-regulated by dioscin, such as C/EBPα and several glycolysis-related proteins including triosephosphate isomerase, cofilin-1 (interaction with triosephosphate isomerase) and phosphoglycerate kinase (Jung et al. 2002). In contrast, dioscin downregulated about twenty proteins in which pyruvate kinase muscle isozymes (PKM) were the most susceptible one. PKM2 is a limiting glycolytic enzyme catalyzing the final step in glycolysis that is crucial in tumor metabolism and growth. Several lines of evidence show that the knockdown of PKM2 inhibits cell proliferation and induces apoptosis in a variety of cancers (Hu et al. 2015); furthermore, upregulation of PKM2 has been demonstrated in prednisolone resistant leukemia (Hulleman et al. 2009), suggesting PKM2 as a therapeutic target. The in-gel digestions and LC-MS/MS determination showed that dioscin down-regulated PKM protein levels. The determination of its functional role on PKM2 needs further investigation.

Conclusion

Our integrated bioinformatics approach reveals the importance of dioscin-induced death receptor related apoptosis, energy metabolic pathways and differentiation induction (Fig. 8). Dioscin exerts its antileukemic effect through the up-regulation of both death ligands and death receptors and a crosstalk activation of mitochondrial apoptosis pathway with the collaboration of tBid and Bak formation. In addition, proteomics approach reveals an altered metabolic signature of dioscin-treated cells and the induction of differentiation of promyelocytes to granulocytes and monocytes in which the C/EBPα plays a key role.

Acknowledgments This work was supported by the grant from the Ministry of Sciences and Technology in Taiwan (MOST 103-2320-B-002-009-MY3 and MOST 106-2320-B-126-001-MY2).

References

Abdel-Hamid NI, El-Azab MF, Moustafa YM (2017) Macrolide antibiotics differentially influence human HepG2 cytotoxicity and modulate intrinsic/extrinsic apoptotic pathways in rat hepatocellular carcinoma model. Naunyn Schmiedeberg's Arch Pharmacol 390:379–395

Baker SJ, Reddy EP (1998) Modulation of life and death by the TNF receptor superfamily. Oncogene 17:3261–3270

Burmistrova O, Perdomo J, Simões MF, Rijo P, Quintana J, Estévez F (2015) The abietane diterpenoid parvifloron D from Plectranthus ecklonii is a potent apoptotic inducer in human leukemia cells. Phytomedicine 22:1009–1016

Cai J, Liu M, Wang Z, Ju Y (2002) Apoptosis induced by dioscin in Hela cells. Biol Pharm Bull 25:193–196

Ejarque-Ortiz A, Tusell JM, Serratosa J, Saura J (2007) CCAAT/enhancer binding protein-alpha is down-regulated by toll-like receptor agonists in microglial cells. J Neurosci Res 85:985–993

Girard N, Tremblay M, Humbert M, Grondin B, Haman A, Labrecque J, Chen B, Chen Z, Chen SJ, Hoang T (2013) RARα-PLZF oncogene inhibits C/EBPα function in myeloid cells. Proc Natl Acad Sci U S A 110:13522–13527

Herst PM, Howman RA, Neeson PJ, Berridge MV, Ritchie DS (2011) The level of glycolytic metabolism in acute myeloid leukemia blasts at diagnosis is prognostic for clinical outcome. J Leukoc Biol 89:51–55

Hoffman B, Amanullah A, Shafarenko M, Liebermann DA (2002) The proto oncogene c-myc in hematopoietic development and leukemogenesis. Oncogene 21:3414–3421

Hu W, Lu SX, Li M, Zhang C, Liu LL, Fu J, Jin JT, Luo RZ, Zhang CZ, Yun JP (2015) Pyruvate kinase M2 prevents apoptosis via modulating Bim stability and associates with poor outcome in hepatocellular carcinoma. Oncotarget 6:6570–6583

Hulleman E, Broekhuis MJ, Pieters R, Den Boer ML (2009) Pyruvate kinase M2 and prednisolone resistance in acute lymphoblastic leukemia. Haematologica 94:1322–1324

Jung J, Yoon T, Choi EC, Lee K (2002) Interaction of cofilin with triosephosp hate isomerase contributes glycolytic fuel for Na,K-ATPase via rho-mediated signaling pathway. J Biol Chem 277:48931–48937

Katz C, Zaltsman-Amir Y, Mostizky Y, Kollet N, Gross A, Friedler A (2012) Molecular basis of the interaction between proapoptotic truncated BID (tBID) protein and mitochondrial carrier homologue 2 (MTCH2) protein: key players in mitochondrial death pathway. J Biol Chem 287:15016–15023

Khan MW, Chakrabarti P (2015) Gluconeogenesis combats cancer: opening new doors in cancer biology. Cell Death Dis 6:e1872

Kim YS, Kim EA, Park KG, Lee SJ, Kim MS, Sohn HY, Lee TJ (2012) Dioscin sensitizes cells to TRAIL-induced apoptosis through down-regulation of c-FLIP and Bcl-2. Oncol Rep 28:1910–1916

Kim EA, Jang JH, Lee YH, Sung EG, Song IH, Kim JY, Kim S, Sohn HY, Lee TJ (2014) Dioscin induces caspase-independent apoptosis through activation of apoptosis-inducing factor in breast cancer cells. Apoptosis 19:1165–1175

Lavrik IN (2014) Systems biology of death receptor networks: live and let die. Cell Death Dis 5:e1259

Lim WC, Kim H, Kim YJ, Choi KC, Lee IH, Lee KH, Kim MK, Ko H (2017) Dioscin suppresses TGF-β1-induced epithelial-mesenchymal transition and suppresses A549 lung cancer migration and invasion. Bioorg Med Chem Lett 27:3342–3348

Lin TC, Hou HA, Chou WC, Ou DL, Yu SL, Tien HF, Lin LI (2011) CEBPA methylation as a prognostic biomarker in patients with *de novo* acute myeloid leukemia. Leukemia 25:32–40

Liu LL, Long ZJ, Wang LX, Zheng FM, Fang ZG, Yan M, Xu DF, Chen JJ, Wang SW, Lin DJ, Liu Q (2013) Inhibition of mTOR pathway sensitizes acute myeloid leukemia cells to aurora inhibitors by suppression of glycolytic metabolism. Mol Cancer Res 11:1326–1336

Ma R, Zhang W, Tang K, Zhang H, Zhang Y, Li D, Li Y, Xu P, Luo S, Cai W, Ji T, Katirai F, Ye D, Huang B (2013) Switch of glycolysis to gluconeogenesis by dexamethasone for treatment of hepatocarcinoma. Nat Commun 4:2508

Masuda Y, Asada K, Satoh R, Takada K, Kitajima J (2015) Capillin, a major constituent of Artemisia capillaris Thunb. flower essential oil, induces apoptosis through the mitochondrial pathway in human leukemia HL-60 cells. Phytomedicine 22:545–552

Muratcioglu S, Presman DM, Pooley JR, Grøntved L, Hager GL, Nussinov R, Keskin O, Gursoy A (2015) Structural modeling of GR interactions with the SWI/SNF chromatin remodeling complex and C/EBP. Biophys J 109:1227–1239

Nerlov C (2004) C/EBPα mutations in acute myeloid leukaemias. Nat Rev Cancer 4:394–400

Ohlsson E, Schuster MB, Hasemann M, Porse BT (2016) The multifaceted functions of C/EBPα in normal and malignant haematopoiesis. Leukemia 30:767–775

Qu X, Zhai Z, Liu X, Li H, Ouyang Z, Wu C, Liu G, Fan Q, Tang T, Qin A, Dai K (2014) Dioscin inhibits osteoclast differentiation and bone resorption through down-regulating the Akt signaling cascades. Biochem Biophys Res Commun 443:658–665

Radomska HS, Jernigan F, Nakayama S, Jorge SE, Sun L, Tenen DG, Kobayashi SS (2015) A cell-based high-throughput screening for inducers of myeloid differentiation. J Biomol Screen 20:1150–1159

Rahman N, Jeon M, Song HY, Kim YS (2016) Cryptotanshinone, a compound of salvia miltiorrhiza inhibits pre-adipocytes differentiation by regulation of adipogenesis-related genes expression via STAT3 signaling. Phytomedicine 23:58–67

Sarosiek KA, Chi X, Bachman JA, Sims JJ, Montero J, Patel L, Flanagan A, Andrews DW, Sorger P, Letai A (2013) BID preferentially activates BAK while BIM preferentially activates BAX, affecting chemotherapy response. Mol Cell 51:751–765

Shen M, Bunaciu RP, Congleton J, Jensen HA, Sayam LG, Varner JD, Yen A (2011) Interferon regulatory factor-1 binds c-Cbl, enhances mitogen activated protein kinase signaling and promotes retinoic acid-induced differentiation of HL-60 human myelo-monoblastic leukemia cells. Leuk Lymphoma 52:2372–2379

Song K, Li M, Xu X, Xuan LI, Huang G, Liu Q (2016) Resistance to chemotherapy is associated with altered glucose metabolism in acute myeloid leukemia. Oncol Lett 12:334–342

Song X, Wang Z, Liang H, Zhang W, Ye Y, Li H, Hu Y, Zhang Y, Weng H, Lu J, Wang X, Li M, Liu Y, Gu J (2017) Dioscin induces gallbladder cancer apoptosis by inhibiting ROS-mediated PI3K/AKT signalling. Int J Biol Sci 13:782–793

Suzuki H, Hisamatsu T, Chiba S, Mori K, Kitazume MT, Shimamura K, Nakamoto N, Matsuoka K, Ebinuma H, Naganuma M, Kanai T (2016) Glycolytic pathway affects differentiation of human monocytes to regulatory macrophages. Immunol Lett 176:18–27

Tao X, Xu L, Yin L, Han X, Qi Y, Xu Y, Song S, Zhao Y, Peng J (2017) Dioscin induces prostate cancer cell apoptosis through activation of estrogen receptor-β. Cell Death Dis 8:e2989

Tenen DG (2003) Disruption of differentiation in human cancer: AML shows the way. Nat Rev Cancer 3:89–101

Tiwari M, Prasad S, Tripathi A, Pandey AN, Ali I, Singh AK, Shrivastav TG, Chaube SK (2015) Apoptosis in mammalian oocytes: a review. Apoptosis 20:1019–1025

Tong Q, Qing Y, Wu Y, Hu X, Jiang L, Wu X (2014) Dioscin inhibits colon tumor growth and tumor angiogenesis through regulating VEGFR2 and AKT/MAPK signaling pathways. Toxicol Appl Pharmacol 281:166–173

Tung CL, Jian YJ, Chen JC, Wang TJ, Chen WC, Zheng HY, Chang PY, Liao KS, Lin YW (2016) Curcumin downregulates p38 MAPK-dependent X-ray repair cross-complement group 1 (XRCC1) expression to enhance cisplatin-induced cytotoxicity in human lung cancer cells. Naunyn Schmiedeberg's Arch Pharmacol 389:657–666

Varfolomeev E, Goncharov T, Fedorova AV, Dynek JN, Zobel K, Deshayes K, Fairbrother WJ, Vucic D (2008) c-IAP1 and c-IAP2 are critical mediators of tumor necrosis factor alpha (TNFalpha)-induced NF-kappaB activation. J Biol Chem 283:24295–24299

Wang X, Huang G, Mei S, Qian J, Ji J, Zhang J (2009) Over-expression of C/EBP-alpha induces apoptosis in cultured rat hepatic stellate cells depending on p53 and peroxisome proliferator-activated receptor-gamma. Biochem Biophys Res Commun 380:286–291

Wang Y, He QY, Chiu JF (2014) Dioscin induced activation of p38 MAPK and JNK via mitochondrial pathway in HL-60 cell line. Eur J Pharmacol 735:52–58

Warburg O, Wind F, Negelein E (1927) The metabolism of tumors in the body. J Gen Physiol 8:519–530

Xu RH, Pelicano H, Zhou Y, Carew JS, Feng L, Bhalla KN, Huang P (2005) Inhibition of glycolysis in cancer cells: a novel strategy to overcome drug resistance associated with mitochondrial respiratory defect and hypoxia. Cancer Res 65:613–621

Yao CJ, Works K, Romagnoli PA, Austin GE (2005) Effects of overexpression of HBP1 upon growth and differentiation of leukemic myeloid cells. Leukemia 19:1958–1968

Yoshida H, Imamura T, Fujiki A, Hirashima Y, Miyachi M, Inukai T, Hosoi H (2012) Post-transcriptional modulation of C/EBPα prompts monocytic differentiation and apoptosis in acute myelomonocytic leukaemia cells. Leuk Res 36:735–741

You M, Jing J, Tian D, Qian J, Yu G (2016) Dioscin stimulates differentiation of mesenchymal stem cells towards hypertrophic chondrocytes *in vitro* and endochondral ossification *in vivo*. Am J Transl Res 8:3930–3938

Zhang C, Peng J, Wu S, Jin Y, Xia F, Wang C, Liu K, Sun H, Liu M (2014) Dioscin promotes osteoblastic proliferation and differentiation via Lrp5 and ER pathway in mouse and human osteoblast-like cell lines. J Biomed Sci 21:30

Zhang G, Zeng X, Zhang R, Liu J, Zhang W, Zhao Y, Zhang X, Wu Z, Tan Y, Wu Y, Du B (2016a) Dioscin suppresses hepatocellular carcinoma tumor growth by inducing apoptosis and regulation of TP53, BAX, BCL2 and cleaved CASP3. Phytomedicine 23:1329–1336

Zhang W, Yin L, Tao X, Xu L, Zheng L, Han X, Peng J (2016b) Dioscin alleviates dimethylnitrosamine-induced acute liver injury through regulating apoptosis, oxidative stress and inflammation. Environ Toxicol Pharmacol 45:193–201

Zhao X, Tao X, Xu L, Yin L, Qi Y, Xu Y, Peng J (2016a) Dioscin induces apoptosis in human cervical carcinoma HeLa and SiHa cells through ROS-mediated DNA damage and the mitochondrial signaling pathway. Molecules 21:E730

Zhao X, Xu L, Zheng L, Yin L, Qi Y, Han X, Xu Y, Peng J (2016b) Potent effects of dioscin against gastric cancer in vitro and in vivo. Phytomedicine 23:274–282

Zheng T, Fu JJ, Hu L, Qiu F, Hu M, Zhu JJ, Hua ZC, Wang H (2013) Nanoarchitectured electrochemical cytosensors for selective detection of leukemia cells and quantitative evaluation of death receptor expression on cell surfaces. Anal Chem 85:5609–5616

Zhou Q, Song W, Xiao W (2017) Dioscin induces demethylation of DAPK-1 and RASSF-1alpha genes via the antioxidant capacity resulting in apoptosis of bladder cancer T24 cells. EXCLI J 16: 101–112